IOCN 2022

MDPI

Proceedings Paper

Self-Assembly of Polydisperse Y-Shaped Polymer Brushes under Good Solvent Conditions †

Petr Fridrich and Zbyšek Posel *

Department of Informatics, Faculty of Science, Jan Evangelista Purkyně University in Ústí nad Labem, Pasteurova 3632/15, 400 96 Ústí nad Labem, Czech Republic; petr.fridrich@ujep.cz

* Correspondence: zbysek.posel@ujep.cz

† Presented at the 3rd International Online-Conference on Nanomaterials, 25 April–10 May 2022; Available online: https://iocn2022.sciforum.net/.

Abstract: Y-shaped polymer brushes contains two homopolymer branches attached at single grafting points. So far monodisperse systems were mostly studied in theory and by simulation. Introducing polydispersity can reveal new options to control the surface morphology. Here, we employ Dissipative Particle Dynamics, vary brush grafting density, composition of the branches and their incompatibility to describe complex behavior of brushes at good solvent conditions. We show that scaling of brush height obtained from simulations agrees with theory and that usual structures, ripple and aggregates, are shown for monodisperse system. Furthermore, we have observed formation of perforated layer instead of ripple structure for polydisperse systems. Finally, increasing the polydispersity leads to widening of PL phase window and asymmetry in phase diagram

Keywords: self-assembly; polydispersity; Y-shaped brush; modeling

Citation: Fridrich, P.; Posel, Z. Self-Assembly of Polydisperse Y-Shaped Polymer Brushes under Good Solvent Conditions. *Biol. Life Sci. Forum* **2022**, *2*, x. https://doi.org/10.3390/xxxxx

Publisher's Note: MDPI stays neutral with regard to jurisdictional claims in published maps and institutional affiliations.

Copyright: © 2022 by the authors. Submitted for possible open access publication under the terms and conditions of the Creative Commons Attribution (CC BY) license (https://creativecommons.org/licenses/by/4.0/).

1. Introduction

Y-Shaped polymer brushes are composed of two incompatible homopolymer branches that are attached to a same grafting pointy on a substrate [1]. Rich variety of system parameters including individual branch lengths, their chemical nature, grafting density etc. leads to unique phase behavior due to the incompatibility of individual branches and due to their response to the outer environment [2]. Structures that assemble on the surface determine its mechanical, electrical or optical properties and have a great potential in variety of modern technological applications. Mixed polymer brushes refer to systems where two or more homopolymers are randomly grafted at the same point which brings not only unique phase behavior but also issues with controlling the uniformity of grafting and reaching the long-range order [3]. Therefore, in Y-shaped brushes, the grafting point can be occupied by just one branch of each type leading to uniform grafting density of each homopolymer and pronounced long-range ordering. In such systems, the previous investigations showed that self-assembly of polymers can produce layered and ripple structures and spherical micelles formed at selective solvent conditions or in melt state. Furthermore, in nonselective solvent, the dimple structure was observed. In experiment, worm-like structures or nearly bicontinuous structures were formed by Y-shaped poly(tert-butyl acrylate) (PtBA)/polystyrene (PS) brushes on the surface of silica particles [4].

In addition, the advances in synthesis allowed researchers to better control and lower the polydispersity of polymers that are prepared experimentally thus bridging the gap between results from theory and simulations where monodisperse systems are mostly described and real polymers that are always polydisperse. In modelling, the polydispersity is modeled via Schulz-Zimm (SZ) distribution that is commonly used for describing the experimental samples [5,6] Recently, the SZ distribution was used to describe the effect

of polydispersity on structure of polymer brushes under equilibrium and non-equilibrium conditions or to describe the shape of density profile in polymer brushes attached to planar solid surface [7]. In this work, we have used SZ distribution to describe the effect of polydispersity on assembly of Y-shaped brushes attached to planar surface and dispersed under good solvent conditions.

2. Methods

2.1. Dissipative Particle Dynamics

Dissipative particle dynamics (DPD) is well-established simulation method suitable for modeling coarse-grained models of polymer chains and has been used to describe phase behavior of polymers including self-assembly of copolymers in melt [8], solutions or near solid surfaces [9]. Moreover, DPD is also suitable for modeling phase behavior of polymeric systems under non-equilibrium conditions [10].

Basic unit in DPD is called bead which represent collection of atoms, molecules or even larger part of chains. Amount of mass that is hidden within one bead is given by coarse-graining approach [11] used to coarse real or fine-grained systems. Rather than coarse-graining real chains and describe specific system, we have used generic model that can capture general behavior of Y-shaped mixed brushes grafted onto flat surface

2.1. Y-Shaped Mixed Brush Grafted onto Flat Surface

Figure 1 shows schematic picture of flat surface grafted by Y-shaped mixed brush. Our coarse-grained model contains two homopolymer branches with A and B beads that are grafted by one end onto same point on the flat surface. Grafting points are distributed randomly on the surface.

Flat surface is represented by collection of "frozen" beads, i.e., they do not move throughout the simulation, with density equal to density of the surrounding fluid. Reflective layer with bounce-back boundary conditions is placed on the interface between surface and the fluid to avoid its unphysical penetration into the surface. Combination of reflective layer and flat surface with density equal to the surrounding fluid neglect unphysical density fluctuations of the fluid near flat surface [12].

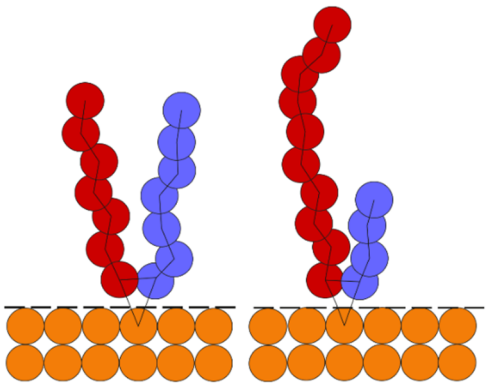

Figure 1. Coarse-grained model of Y-shaped mixed brushes. **Left** picture shows Y-shaped brush with symmetric distribution while **right** picture shows asymmetric distribution of A (red) and B (blue) chain lengths. Orange beads represent frozen wall beads that do not move throughout the simulation and dashed line is reflective layer with bounce-back boundary conditions that avoids penetration of surrounding fluid (not shown here) into the solid surface.

2.3. Polydisperse Y-Shaped Mixed Brushes

We have adopted Schulz-Zimm distribution $P(N)$ [5,6] to include polydispersity to our coarse-grained model. This distribution is frequently used to describe polydispersity in simulations and corresponds to results in synthesis [13]. Delta function $\Gamma(k)$ and two

parameters N_n and k are used to describe distribution of chain lengths N in Equation (1).

$$P(N) = \frac{k^k N^{k-1}}{\Gamma(k) N_n} e^{\left(-k\frac{N}{N_n}\right)}. \quad (1)$$

Here, the N_n is the number averaged chain length and k is linked to polydispersity index via relation $PDI = N_w/N_n = 1 + 1/k$. In case of monodisperse system, the $k \to \infty$, and $P(N)$ transforms to delta function while for $k \to 1$ the distribution of chain lengths has exponentially decaying shape. A branch is kept monodisperse in the rest of the paper while B branch has individual polydispersity $PDI = \{1; 1{,}1; 1.5; 2.0\}$ to cover low and high polydisperse systems, respectively. These polydispersity indexes are also available experimentally.

3. Results

3.1. Monodisperse Y-Shaped Brush Scaling

We start our discussion with monodisperse systems where we validate our simulation model. First, to identify systems of interest we performed simulations of monodisperse systems equal compositions, $f_{AB} = 0.5$. We varied grafting density from 0.01 up to 1.5. Figure 2 shows height of the brush H as a function of grafting density σ.

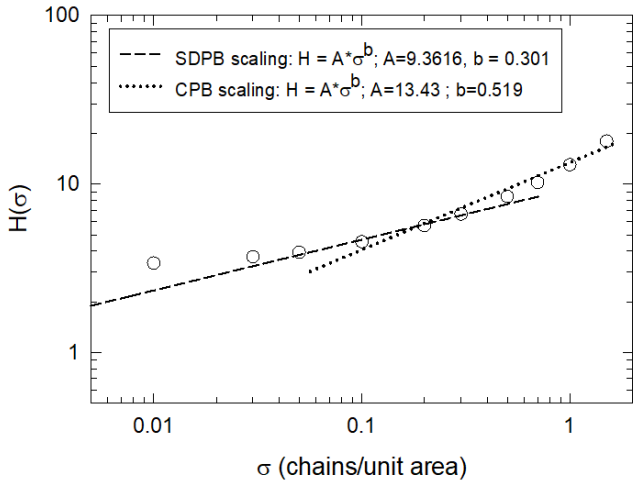

Figure 2. Brush height H as a function of grafting density σ for Y-shaped mixed brushes with symmetric composition $f_{AB} = 0.5$. Dashed line indicates scaling of semi-dilute polymer brush (SDPB) regime while dotted line stands for concentrated polymer brush (CPB) regime

We clearly see that systems with low grafting density, $\sigma \leq 0.03$ deviates from Semi-dilute polymer brush regime (SDPB) scaling (dashed line) and brushes are well in mushroom regime. Increasing the σ to 0.1 leads to crossover regime between mushroom and SDPB, while further increase to 0.5 leads to crossover between SDPB and CPBD regimes. System with $\sigma > 0.5$ have all chains well in CPB. Scaling behavior of the brush height in Figure 2 agrees with those published before [14] and allowed us to select appropriate grafting densities for each regime and construct their phase diagrams. In the rest of the paper, we show phase diagrams for $\sigma = \{0.03; 0.1; 0.5; 1.0\}$, if not said otherwise.

3.2. Phase Behvaior of Monodisperse Y-Shaped Brush

Figure 3 shows complete phased diagrams of monodisperse Y-shaped copolymer brushes under good solvent conditions for both branches that are grafted onto flat surface. Grafting densities corresponds to those selected from Figure 2 where Figure 3a shows

results for $\sigma = 0.03$, Figure 3b for $\sigma = 0.10$, Figure 3c for $\sigma = 0.50$ and Figure 3d for $\sigma = 1.0$, respectively. Phase diagrams are displayed in a_$a_{AB} - f_{AB}$ plane, where a_{AB} shows incompatibility between A and B branch in Y-shaped brush and f_{AB} shows brush composition. Phase diagrams are symmetric around $f_{AB} = 0.5$, where left part of the diagram shows results for A branch and right part for B branch of the brush.

Only aggregates, that can potentially transform into different type of micelles under different solvent conditions, are formed in system with low grafting density, $\sigma = 0.03$, in Figure 3a, where chains are in mushroom regime. Here, the aggregates form mostly isolated islands that can temporarily interconnect. For $f_{AB} \neq 0.5$ cases, the stability of aggregates is very poor and results in disorder phase. Increasing the grafting density to the crossover value between mushroom and SDPB regime, $\sigma = 0.1$ and Figure 3a, drives assembly of ripple structure at $f_{AB} = 0.5$ and shift of aggregate phase window outside the symmetric region. Although ripple structure is stable it is still prone to fluctuations caused by surrounding fluid. On the other hand, aggregates that are formed close to symmetric case seems stable enough. Again, here we do not observe formation of any micellar structures since both branches of the brush are dispersed under good solvent conditions.

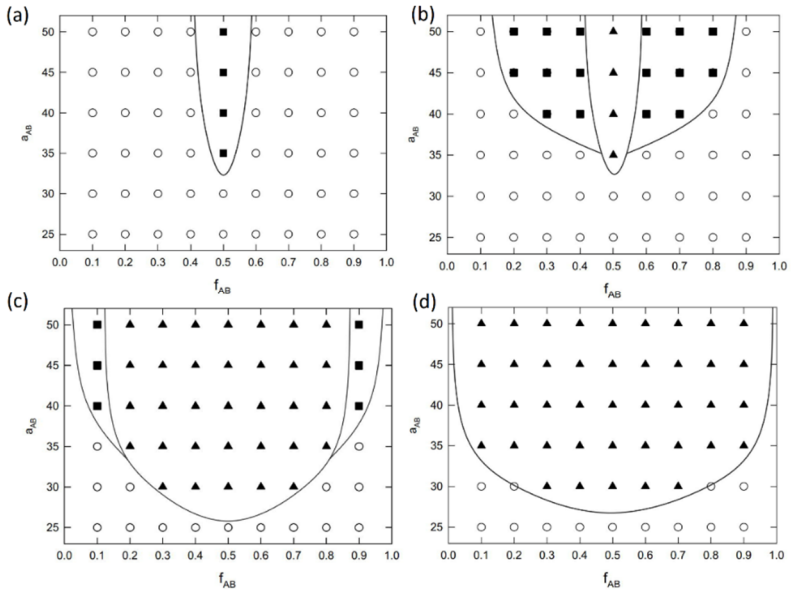

Figure 3. Phase diagrams of monodisperse Y-shaped mixed brushed under good solvent conditions grafted onto flat surface with (**a**) $\sigma = 0.03$, (**b**) $\sigma = 0.10$, (**c**) $\sigma = 0.50$ and (**d**) $\sigma = 1.0\ chains/unit\ area$ grafting density. Phase diagrams are shown in $a_{AB} - f_{AB}$ plane, where a_{AB} shows incompatibility between A and B branch in Y-shaped brush and f_{AB} shows composition of the branches in the brush. Symbols: disordered systems (open circle), aggregates (filled square), ripple structure (filled triangle). Solid line shows approximate boundaries between different phases.

Further increase of grafting density to $\sigma = 0.5$ brings chains to crossover between SDPB and CPBD. The phase diagram in Figure 3c shows significant broadening of ripple phase window and aggregates are pushed to outskirt of phase diagram. Moreover, we see that order-disorder transition decreased from $a_{AB} = 33$ to a_{AB} around 25 which is close to the value of $\chi_{AB} = 10.5$ predicted for order-disorder transition for pure diblock copolymer melt. Systems with highest grafting density, $\sigma = 1.0$ shows only ripple phase while any other type of structure is not observed.

3.3. Polydisperse Y-Shaped Brush Scaling

To set up proper minimum and maximum chain lengths in Schulz-Zimm distribution and to test the validity of generated polydisperse set of chains, we first compare scaling behavior of polydisperse homopolymer brush H scaled by corresponding monodisperse brush H_{mono}. Figure 4 shows scaled brush height H/H_{mono} as a function of $(PDI-1)^{1/2}$ for all grafting densities considered in this study. We have measured scaled brush height in systems with $PDI = \{1.1,1.3,1.5,1.8,2.0\}$. Solid black line in the figure shows linear scaling predicted by theory in form

$$H/H_{mono} = 1 + \alpha(PDI-1)^{1/2}, \quad (2)$$

where $\alpha \approx 1.0$ [7] and color points mark our simulation results. We see that our systems follow theoretical predictions in case that minimum and maximum chain lengths in our system are 5, and $6\langle N\rangle$, respectively. These settings are used in rest of the paper for all polydisperse systems and determine the size of simulation box. Moreover, we see, that scaling is achieved for chains with medium and high grafting density with chains well in SDPB or CPBD regime (see Figure 2 for details). Chains at $\sigma = 0.03$ that are in mushroom regime have $\alpha \approx 0.55$.

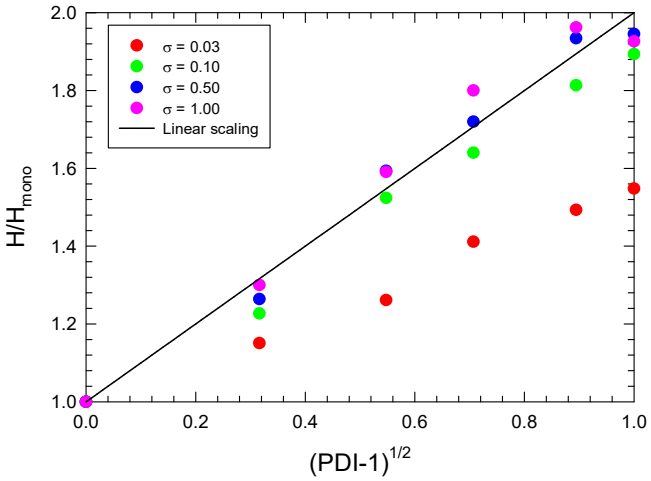

Figure 4. Brush height of polydisperse homopolymer brush H scaled by corresponding monodisperse value H_{mono}, as a function of polydispersity index $PDI = N_w/N_n$. Solid line indicates linear scaling predicted by theory and colored points are simulation results for different grafting densities.

3.4. Phase Behvaior of Polydisperse Y-Shaped Brush

Figure 5 shows phase behavior of polydisperse brushes with low polydispersity $PDI = 1.1$. Comparison with monodisperse systems in Figure 3 reveal that even small polydispersity of B branch influence the assembly in the system and surface morphology. First, we see that no assembly is observed in case of sparsely grafted Y-shaped brushes ($\sigma = 0.03$ phased diagram is not shown here) and suppress the formation of ripple phase in systems with $\sigma = 0.1$ where we see only the aggregates. More importantly, in system with medium ($\sigma = 0.5$) to high grafting density ($\sigma = 1.0$), we see formation of perforated layer (PL) of A instead of ripple structure formed in monodisperse system. The PL phase extends further to $f_{AB} = 0.6$. The reason for that lies in long polydisperse B branches that stick out from B ripple phase located close to the surface. These chains then penetrate through the A phase to the surrounding fluid. Such long chains are not in monodisperse systems where all B branches are, for $f_{AB} > 0.5$ shorter than A ones. Therefore, similar behavior is not observed in case $f_{BA} > 0.5$ where monodisperse A branches are much shorter and not able to penetrate B layer. For that reason, the phase diagrams of polydisperse systems are no longer symmetric around $f_{BA} = 0.5$.

Further increasing of PDI to 1.5 and 2.0, figures not shown here, moves the barrier between order-disorder transition above systems with $\sigma = 0.1$. Moreover, the formation of PL phase is more pronounced, ranges from 0.5 up to 0.7 and occupies large portion of B phase window, where in monodisperse system we see compact A layer above B ripple phase. Finally, we plot in Figure 6 simulation snapshots of ripple and PL phase formed in monodisperse and polydisperse ($PDI = 1.1$) systems with $\sigma = 0.5$ and $f_{AB} = 0.5$.

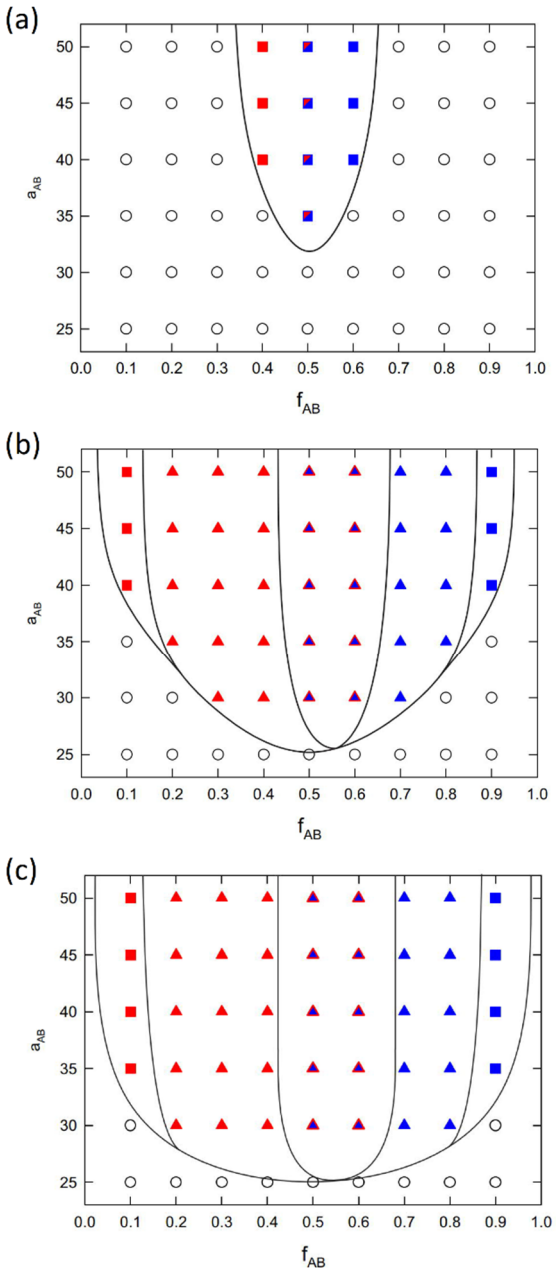

Figure 5. Phase diagrams of polydisperse Y-shaped mixed brushed with $PDI = 1.1$ under good solvent conditions grafted onto flat surface with (**a**) $\sigma = 0.10$, (**b**) $\sigma = 0.50$ and (**c**) $\sigma = 1.0$ $chains/unit\ area$ grafting density. Phase diagrams are shown in $a_{AB} - f_{AB}$ plane, where a_{AB} shows incompatibility between A and B branch in Y-shaped brush and f_{AB} shows composition of the branches in the brush. Symbols: disordered systems (open circle), aggregates (filled square), ripple structure (filled triangle). Solid line shows approximate boundaries between different phases. Red color shows structures formed by A branch and blue color stands for B branch. Half red, half blue

square indicates that both types form aggregates and blue triangle with red edge line indicates perforated layer.

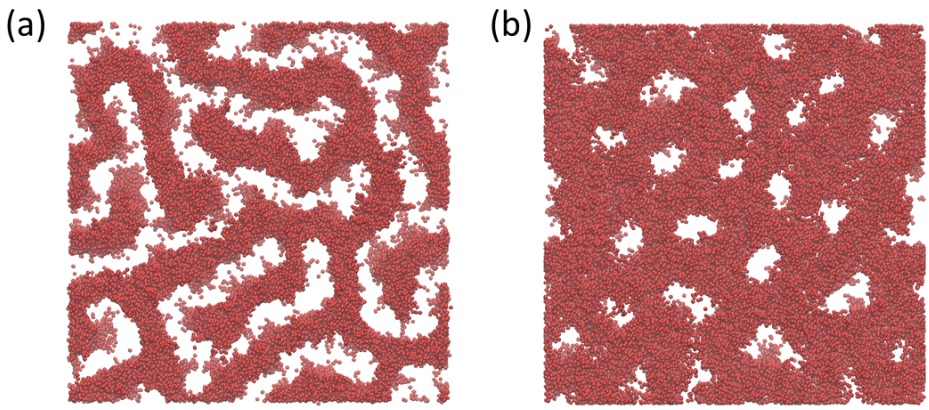

Figure 6. Simulation snapshots of (**a**) ripple phase formed in monodisperse system and (**b**) perforated layer formed in polydisperse system with $PDI = 1.1$. Both systems have $\sigma = 0.5$ and $f_{AB} = 0.5$. Red color stands for A branch of Y-shaped brush. The polydisperse B branch is omitted for clarity.

3. Discussion

In this work, we employed coarse-grained modelling and Dissipative particle dynamics to describe the phase behavior of polydisperse Y-shaped brushes grafted to flat surface and dispersed under good solvent conditions. In our polydisperse brush, the A branch is kept monodisperse while B branch possess different polydispersity that fits experimentally achievable values. First, we have validated our model by fitting the scaling behavior of monodisperse system as a function of grafting density. We show that our model successfully captures all scaling regimes from mushroom to concentrated polymer brush and we were able to set proper grafting densities in these regimes for further simulations. Then, we performed series of simulations to describe phase behavior of monodisperse systems and show that only aggregates and ripple structures are formed which agrees with previous simulation studied and with theoretical predictions. Furthermore, we consider Schulz-Zimm distribution to include polydispersity to B branch of Y-shaped brush We show, that even small polydispersity shifts order-disorder transition to higher grafting densities. More importantly, we show that starting at $PDI = 1.1$ the ripple structure is replaced by perforated layer and that its phase window extends more with increasing the PDI up to 2 where only ripple and perforated layer are observed. Finally, we show that manipulating with polydispersity of branches in Y-shaped brush can lead to interesting phase behavior and that combinations of polydispersity can offer additional parameter to control the morphology of functionalized surface.

Author Contributions: P.F. and Z.P. performed the simulations. P.F. was responsible for writing the software for analyzing the trajectories and for data curation. Z.P. wrote and edited the manuscript. All authors have read and agreed to the published version of the manuscript.

Funding: ZP acknowledges the support from ERDF/ESF project "UniQSurf-Centre of biointerfaces and hybrid functional materials "(No. CZ.02.1.01/0.0/17_048/0007411). ZP and PF both acknowledge the assistance provided by the Technology Agency of the Czech Republic, under the project Metamorph, project No. TO01000329.

Institutional Review Board Statement: Not applicable

Informed Consent Statement: Not applicable

Conflicts of Interest: The authors declare no conflict of interest.

References

1. Hou, W.; Liu, Y.; Zhao, H. Surface Nanostructures Based on Assemblies of Polymer Brushes. *ChemPlusChem* **2020**, *85*, 998–1007.
2. Li, M.; Pester, C.W. Mixed Polymer Brushes for "Smart" Surfaces. *Polymers* **2020**, *12*, 1553–1580.
3. Yin, Y.; Jiang, R.; Wang, Z.; Li, B. Influence of Grafting Point Distribution on the Surface Structures of Y-Shaped Polymer Brushes in Solution. *Langmuir* **2016**, *32*, 7467–7475.
4. Zhao, B.; Zhu, L. Nanoscale Phase Separation in Mixed Poly(tert-butyl acrylate)/Polystyrene Brushes on Silica Nanoparticles under Equilibrium Melt Conditions. *Am. Chem. Soc.* **2006**, *128*, 4574–4575.
5. Schulz, G.V. Uber Die Kinetik Der Kettenpolymerisationen. *Phys. Chem.* **1939**, *43*, 25–46.
6. Zimm, B. Apparatus and methods for measurement and interpretation of the angular variation of light scattering; preliminary results on polystyrene solutions. *J. Chem. Phys.* **1948**, *16*, 1099–1116.
7. Qi, S.H.; Klushin, L.I.; Skvortsov, A.M.; Schmid, F. Polydisperse Polymer Brushes: Internal Structure, Critical Behavior, and Interaction with Flow. *Macromolecules* **2016**, *49*, 9665–9683.
8. Posel, Z.; Lísal, M.; Brennan, J.K. Interplay between microscopic and macroscopic phase separations in ternary polymer melts: Insight from mesoscale modelling. *Fluid Phase Equilib.* **2009**, *283*, 38–48.
9. Posel, Z.; Posocco, P. Tuning the Properties of Nanogel Surfaces by Grafting Charged Alkylamine Brushes. *Nanomaterials* **2019**, *9*, 1514–1527.
10. Posel, Z.; Svoboda, M.; Coray, C.; Lisal, M. Flow and aggregation of rod-like proteins in slit and cylindrical pores coated with polymer brushes: An insight from dissipative particle dynamics. *Soft Matter* **2017**, *13*, 1634–1645.
11. Brin, E.; Algaer, E.A., Ganguly, P.; Li, C.; Rodriguez-Ropero, F.; Van der Vegt, N.F.A. Systematic coarse-graining methods for soft matter simulations—A review. *Soft Matter* **2013**, *9*, 2108–2119.
12. Pivkin, I.V.; Karniadakis, G.E. A new method to impose no-slip boundary conditions in dissipative particle dynamics. *J. Comput. Phys.* **2005**, *207*, 114–128.
13. Turgman, C.S.; Srogl, J.; Kiserow, D.; Genzer, J. On-demand degrafting and the study of molecular weight and grafting density of Poly(methyl methacrylate) brushes on flat silica substrates. *Langmuir* **2015**, *31*, 2372–2381.
14. Gao, H.M.; Liu, H.; Lu, Z.Y.; Sun, Z.Y.; An, L.J. The structures of thin layer formed by microphase separation of grafted Y-shaped block copolymers in solutions. *J. Chem. Phys.* **2013**, *138*, 224905–224914.